Front. Mater. Sci. 2024, 18(4): 240700
https://doi.org/10.1007/s11706-024-0700-1

REVIEW ARTICLE

Graphene oxide-based nanohybrids incorporated in nanofiltration and reverse osmosis membranes for desalination and dye separation: a review

Iluska Marques Santos (✉) and Carlos Alberto Caldas de Souza

Graduate Program in Chemical Engineering (PPEQ), Universidade Federal da Bahia, Salvador, Bahia, Brazil

ABSTRACT: Novel advanced nanocomposites formed by associating graphene oxide (GO) nanosheets with other nanomaterials such as titanium dioxide nanoparticles, cellulose nanofibers, cellulose nanocrystals, and carbon nanotubes were incorporated in nanofiltration (NF) and reverse osmosis (RO) membranes for wastewater treatment and desalination. GO-based nanocomposite has promising potential in membrane technology due to its high hydrophilicity, absorption capacity, good dispersibility in water and organic solvents, anti-biofouling properties, and negative charge. Moreover, additional properties can be obtained depending on the nanohybrid formed. This review paper highlights the recent breakthrough in membranes functionalized with GO-based nanohybrids, focusing on membrane performance in terms of permeability, selectivity, and antifouling properties. Although GO-based nanohybrids have made significant progress in membrane technology, improvements are still needed, especially regarding trade-off effects. Furthermore, the studies presented here are limited to laboratory scale, which leads to suggestions for new studies evaluating the possibility of commercial application and the potential environmental impact caused by nanocomposites.

KEYWORDS: graphene oxide-based nanohybrid; membrane performance; nanofiltration; reverse osmosis

Contents

Received June 12, 2024; accepted September 18, 2024

E-mail: iluska.santos@ufba.br

1 Introduction

"Water is a basic human right." This declaration was made by the United Nations (UN) at the General Assembly in 2010. However, this resource is not so easy to access in some communities. People in various parts of the world continue to struggle to access clean water and, in some cases, can only obtain it through inhumane, environmentally harmful, or costly means [1]. Perspectives indicate that water supply will be even more difficult in the coming years. In 2018, the World Economic Forum ranked the water crisis among the top three problems in the world [2]. Unregulated urbanization, climate change, increasing population growth, industrialization, and agricultural expansion have been cited as the main causes of this shortage [3–5].

Several solutions have been developed as strategies to minimize water crises. In this scenario, water treatment using membrane separation technology through nanofiltration (NF) and reverse osmosis (RO) processes is attracting worldwide attention due to its high separation efficiency, easy operation, and large water treatment capacity [6]. RO membranes are highly efficient in removing monovalent salts from water and have been widely used for seawater desalination. However, the RO process requires high operating pressures, and the water permeability is generally low [7]. On the other hand, NF membranes are highly efficient in wastewater treatment and are considered the most promising option for dye removal [8]. Additionally, NF membranes have larger pores than RO membranes, resulting in higher water flux and milder operating pressure conditions [9]. Although RO and NF membranes have gained wide acceptance in the industry, scientists are looking forwards to further improving efficiency by incorporating nanomaterials into the membrane structure [8].

There are several ways to incorporate nanomaterials into the membrane surface or polymer matrix. In mixed matrix membranes (MMMs), nanomaterials are added to the polymer solution during the polymer casting step. After the solution casting and phase inversion process, a membrane is formed with nanomaterials dispersed in its matrix [10]. In flat sheet membranes, one of the most regularly used strategies to incorporate nanomaterials into the membrane surface is the vacuum filtration method [11]. In thin-film composite (TFC) membranes, usually, the nanomaterials are incorporated into the polyamide (PA) layer during its synthesis by interfacial polymerization (IP) processes between two highly reactive monomers [12]. TFC membranes with embedded nanomaterials are often called thin-film nanocomposite (TFN) membranes [13].

Studies show that when nanomaterials are added to membranes at the appropriate size, shape, porosity, and concentration, the nanostructures can improve the morphological characteristics of NF and RO membranes and significantly increase their permeability, selectivity, and antifouling properties [6,14]. For example, when titanium dioxide (TiO_2) nanoparticles (NPs) were incorporated into RO membranes, an increase in the hydrophilicity of the membrane surface was observed, resulting in improved permeability, selectivity, and antifouling properties [15]. Furthermore, it may be possible to provide additional functionality to the membranes. Studies with silver NPs, a commonly used antimicrobial agent, have improved the membrane's anti-biofouling properties [16]. Gold and iron oxide NPs are particularly suitable for removing heavy metals from the membrane surface [13], and graphene oxide (GO) is widely used for desalination [17].

Although single nanomaterials can improve some membrane properties, they cannot provide all the benefits simultaneously [18]. It has been proposed that hybrid nanomaterials can combine their properties to give membranes even more significant performance [19]. GO has been attracting attention as an excellent nanomaterial for forming hybrid nanocomposites due to its sheet-like structure that allows it to be uniformly decorated by several other nanostructures [20]. Previous studies have shown that GO-based nanohybrids are highly efficient in improving the membrane surface properties as well as membrane performance [19,21]. However, to the best of our knowledge, there is still no literature on the effectiveness of various GO-based hybrid nanomaterials incorporated into membranes, and the majority of previously published reviews and research articles are focused on the incorporation of a single GO or another

single NP into membranes [12,22]. The few review articles on GO-based nanohybrids have been confined to discussing only the incorporation of the GO/TiO_2 nanocomposite into membranes [23–24]. Therefore, this article aims to provide a comprehensive review of the impact of GO-based nanohybrid on the performance of NF and RO membranes applied in desalination and wastewater treatment processes, mainly focusing on water flux, selectivity and fouling resistance, addressing the latest advances in hybrid nanocomposites formed by the association of GO with TiO_2, carbon nanotubes (CNTs), cellulose nanocrystals (CNCs) and cellulose nanofibers (CNFs), comparing the performance of membranes with different nanomaterials and analyzing how each nanocomposite influences the membrane performance. Furthermore, future perspectives are also discussed.

2 Membrane fouling mitigation

The accumulation of organic, inorganic, and particulate matter on the membrane surface or within its pores remains one of the main challenges of membrane technology [25–26]. This accumulation of unwanted materials, known as fouling, occurs during the membrane separation process, resulting in the formation of a foulant layer on the top of the membrane and pore obstruction, which reduces the permeate flux and the membrane lifespan. In addition, the occurrence of fouling can also require greater operating pressure and increasing energy consumption [27–28]. Generally, physical cleaning (e.g., forward flushing, backwashing, or air sparging) and chemical cleaning (e.g., chlorine-based) are strategies used to remove membrane fouling [25]. However, physical cleaning requires long-term washing and is less efficient when compared to chemical cleaning. On the other hand, chemical cleaning can cause severe damage to membranes due to the use of acids, alkalis, and oxidants [29].

Polymer-based membranes are susceptible to fouling due to surface properties such as inherent hydrophobicity, roughness, and electrical charge [30–32]. Recent studies have recognized that modifying membrane surfaces by incorporating nanomaterials may be an efficient approach to improve the above properties. Generally, the membrane surface is rough. For example, in the case of TFC membranes, the polyamide surface has a rugged structure with ridge-and-valley characteristics, making it easier for fouling to accumulate on the valleys. On the other hand, membranes with a smoother surface tend to accumulate less fouling. Figure 1 shows the schematic behavior of fouling in TFC membranes with rough and smooth surfaces. According to the literature, nanomaterials could likely reduce the roughness by aligned self-assembly on the membrane surface, making it smoother and less prone to material accumulation [33–34]. Furthermore, the literature suggests that hydrophilic nanostructures can enhance membrane hydrophilicity by forming a hydration layer on the membrane surface, preventing the adsorption of undesirable materials [35].

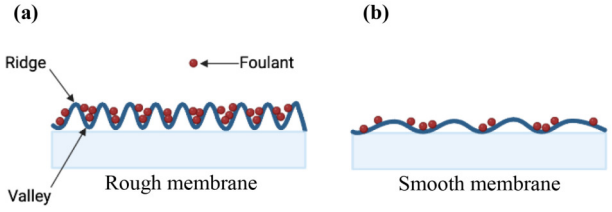

Fig. 1 Schematic model of fouling accumulation in TFC membranes: (**a**) membrane with high surface roughness and high fouling; (**b**) membrane with low surface roughness and low fouling.

The membrane surface charge also plays an important role in the antifouling performance since the surface adsorption of foulants is mainly caused by intramolecular forces or electrostatic interaction between the membrane surface charge and the solute [36]. Repulsive interactions between the negatively charged membrane surface and negatively charged fouling materials also can mitigate fouling [32]. NF and RO membranes have accomplished significant advances through nanotechnology, and many nanomaterials can create innovative solutions to fouling problems [37–38]. Various hydrophilic nanomaterials in single and hybrid configurations were incorporated into NF and RO membranes, and the results showed that the antifouling performance of the membranes was significantly improved. Table 1 summarizes different nanostructures used to functionalize NF and RO membranes and the effects on the hydrophilicity, roughness, and surface charge of membranes [6,39–43].

3 Graphene oxide properties

3.1 Structure and properties of graphene oxide

The application of graphene nanostructures and their derivatives in separation membranes has gained prominence in the scientific community. As shown in

Table 1 Comparison of antifouling performances and surface characteristics of RO and NF membranes with different nanomaterials incorporated [6,39–43]

Nanomaterial	Membrane	Antifouling properties and performances compared to pure membrane	Ref.
GO	RO membrane synthesized by IP	Antibiofouling tests found that increasing the concentration of GO within the membrane PA layer improved their antifouling properties and membrane surface properties, such as hydrophilicity, negative charge, and surface smoothness.	[39]
	NF membrane synthesized by IP	Characterization indicated that the GO membrane exhibited increased hydrophilicity and negative charges. However, there was also a slight increase in surface roughness. Antifouling tests showed that the GO membranes showed greater resistance to biofouling.	[40]
MWCNT	NF membrane synthesized by vacuum filtration and IP	The contact angle tests showed nearly identical results between the pure membrane and the MWCNT membrane. However, the surface roughness of the MWCNT membrane was improved. The antifouling performance tests indicated that the MWCNT membrane was effective in reducing BSA fouling.	[41]
CNC	RO membrane synthesized by IP	The CNC membranes showed better hydrophilicity. However, greater roughness. In the antifouling tests, the CNC membrane showed an 11% lower reduction in water flux compared to the pure membrane, indicating that CNC can improve the fouling resistance of the membranes.	[42]
GO/MWCNT	NF membrane synthesized by IP	Although the GO/MWCNTs membrane exhibited greater roughness, the contact angle decreased significantly from 57.2° for the pristine membrane to 23.4° for the GO/MWCNTs membrane, indicating an improvement in hydrophilicity after nanohybrid incorporation. Antifouling tests revealed that the GO/MWCNTs hybrid nanomaterials enhanced antifouling properties of the membranes.	[6]
GO/TiO_2	NF membrane synthesized by IP	The incorporation of GO/TiO_2 significantly improved the membrane hydrophilicity, and up to a certain concentration also improved the surface roughness. Tests proved that the GO/TiO_2 membrane presented better antifouling performance.	[43]

Fig. 2(a), graphene consists of a two-dimensional (2D) structure, composed of a single atomic layer of sp^2-bonded carbon atoms, with each atom bonded to three others in a honeycomb lattice [44–46]. Such a structure makes this material extremely strong, very conductive, and a million times thinner than paper. However, graphene is a hydrophobic material, which is not desirable for many applications [47]. GO is a derivative of graphene, and both materials have similar structures. Recently, the main route used for the synthesis of GO is the Hummer's method, developed by Hummers and Offeman [48], and consists of the oxidation and exfoliation of graphite powders [47]. During the GO synthesis, functional groups such as hydroxyl, epoxy, carboxyl, and carbonyl can be introduced due to the oxidation conditions. The inclusion of these groups in the basal planes and edges of GO contributes to improving its characteristics, such as chemical stability and hydrophilicity, which facilitates its dispersion in water and polar organic solvents [17,49]. Although the GO structure has been the subject of numerous investigations, it is not fully understood yet. Figure 2(b) illustrates the Lerf–Klinowski model, which was first proposed in 1998 [50–51] and has now been widely accepted as the most likely structure of GO. Compared with graphene, GO has low production costs, large-scale production, and easy processing [52]. Besides, it has been revealed that GO has a high surface area together with antibacterial properties, which are highly advantageous for improving membrane properties [53–54].

In recent efforts to improve membrane performance, GO nanosheets have been embedded either on the surface or within the membrane polymer matrix. Different studies indicate that membranes modified with GO nanosheets showed better hydrophilicity, greater water flux, and antifouling properties due to the presence of functional groups and nanoporous channels in the GO structure [55–57].

3.2 NF and RO membranes incorporated with GO-based nanohybrids

The incorporation of different nanostructures into GO nanosheets has been investigated as a promising strategy to increase membrane performance [58]. Due to their 2D lamellar structure, GO nanosheets serve as a versatile platform for other nanostructures to disperse uniformly on their surface, contributing to GO as an excellent nanomaterial for the formation of nanohybrids [20]. Furthermore, since no single nanomaterial can provide all the beneficial properties simultaneously, when GO is functionalized with other nanostructures, the advantages of both are combined to produce unique properties enhancing the membranes performance [18]. For instance, since the GO interlayer spacing is ~0.80 nm, the space size does not allow sufficient water transport [59–60]. The incorporation of the nanomaterial with appropriate morphology, size, and accommodation when associated with GO can increase the spacing between GO interlayers, promoting greater water mobility [61–64]. Figure 3

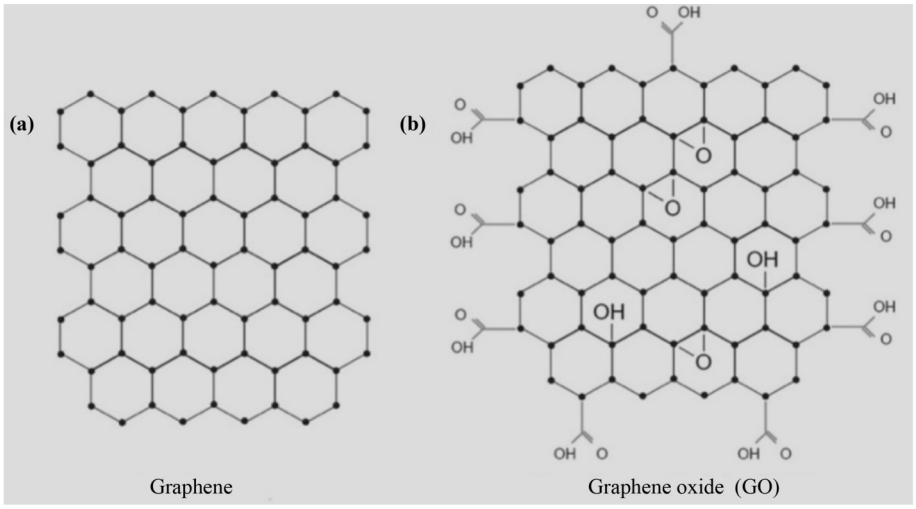

Fig. 2 Most likely structures of (**a**) graphene and (**b**) GO. Reproduced with permission from Ref. [46].

illustrates the mechanism that drives the molecular transport across the membrane with a single GO incorporated and the membrane functionalized with GO-based nanohybrid [65]. Based on this perspective, GO has been combined with several other nanomaterials such as metal and metal-oxide nanostructures, biopolymers, and carbon nanomaterials to create nanohybrids with enhanced properties and capable of improving the membrane performance for seawater and wastewater treatment. When incorporated into the membrane in optimal size and concentration, it is expected that the nanohybrid could be highly efficient in improving water permeability without sacrificing salt rejection. However, if the concentration of nanomaterial is too high, their distribution on the membrane will be uneven, increasing the possibility of damage to the membrane structure due to nanocomposite agglomeration and reducing the membrane rejection ability [58].

4 Graphene oxide-based hybrid nanomaterials incorporated in membranes

4.1 Graphene oxide with metal-oxide nanostructures

4.1.1 Graphene oxide with titanium dioxide (GO/TiO_2)

TiO_2 nanoparticles are chemically stable, hydrophilic, and exhibit high reactivity and photocatalytic activity [66–67]. These properties are essential for the satisfactory performance of nanocomposite membranes since hydrophilicity favors the membrane's permeability, self-cleaning, and antifouling capacity, including resistance to biofouling [68]. Besides, TiO_2 is also non-toxic and available in abundance [19]. NF and RO membranes containing GO/TiO_2 have been intensively studied, specifically in recent years. Previous research records that the incorporation of these nanocomposites complements the selectivity of salts such as NaCl and Na_2SO_4, as well as the retention of hydrocarbons and dyes, in the same way, providing better water permeation [59,66]. Furthermore, incorporating GO/TiO_2 nanocomposites into the PA layer of TFC membranes could result in smoother surfaces and, consequently, make the membrane less prone to fouling [66]. This behavior is related to the GO/TiO_2 auto-deposition on the ridge-and-valley structure of the membrane surface.

In a study by Al-Gamal et al. [66], GO was loaded with TiO_2 to create a nanohybrid with enhanced properties. The membranes were synthesized using an IP method in the absence of nanomaterials and the presence of one, four, and eight PA layers containing GO/TiO_2. In the permeation test, it was noticed that the water flux was improved by increasing the coating layers. At a pressure of 10 kPa, the bare membrane showed a flux of about 40.5 $L \cdot m^{-2} \cdot h^{-1}$, and under the same operation conditions, the membranes with one layer of coating increased the water flux to 46 $L \cdot m^{-2} \cdot h^{-1}$, while the membrane with eight layers of coating increased the water flux by 50% more than that of the bare membrane. Increased membrane water flux caused by the incorporation of nanomaterials in the PA layer has been demonstrated in previous studies, and it has been suggested that

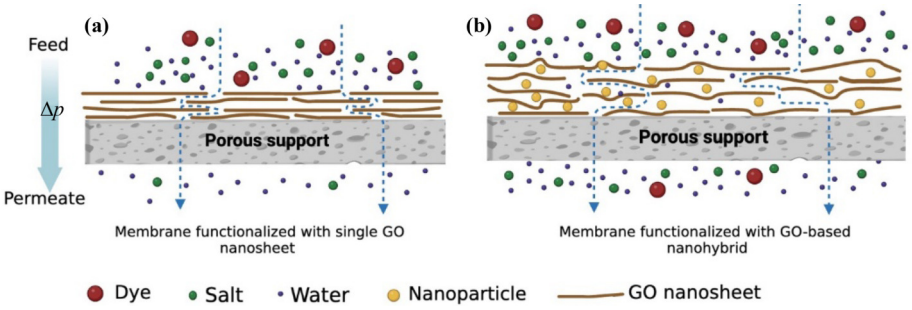

Fig. 3 Molecule transport process mechanisms on (**a**) the membrane with single GO and (**b**) the membrane with GO-based nanocomposites. Reproduced from Ref. [65] with permission of Elsevier.

nanomaterials with highly hydrophilic functional groups could transfer their properties to the membrane, thus improving water–membrane interactions [63]. For example, in the study of Ref. [15], it was observed through contact angle characterization that TiO_2 improved the hydrophilicity of the membrane, which was reflected in the increased water flux. Increasing the distance between GO nanosheet layers could also explain the improvement in permeability. Probably, TiO_2 was placed between GO nanosheet interlayers, which might have increased the GO interlayer distance and, thereby formed larger water channels that could transport water molecules more easily. The same behavior was observed in the study of Ref. [69], where chitosan NPs were incorporated into GO, increasing the GO interlayer spacing resulting in membranes with improved permeability. Increasing the layers of coating and consequently, the concentration of GO/TiO_2 onto the membrane surface also showed high efficiency in salt separation, increasing the NaCl rejection from 81% to 97% and the Na_2SO_4 rejection from 86% to 97%. The GO/TiO_2 nanocomposite exhibited a significantly high negative charge [19]. Consequently, the rejection of salt ions could be driven predominantly by the Donnan exclusion mechanism since the incorporation of these nanocomposites increased the number of negative charges on the membrane surface, resulting in a high electrostatic repulsion force between the membrane surface and anions of Cl^{2-} and SO_4^{2-} [3]. So, the salt rejection can be enhanced when the number of GO/TiO_2 layers increases due to the increased negative charge on the membrane surface. Table 2 shows the comparison in values of permeation flux and retention of NaCl obtained on NF and RO membranes in the absence and presence of GO/TiO_2 [19,66,70].

In the study of Safarpour et al. [19], RO membranes were fabricated using the IP method incorporating various concentrations of reduced-graphene oxide/TiO_2 (rGO/TiO_2) in the PA layer. In both water flux and salt removal tests, membranes with a composition of 0.02 wt.% rGO/TiO_2 were found to be more efficient since the water permeability was improved from 34.3 to 51.3 $L \cdot m^{-2} \cdot h^{-1}$, and the NaCl rejection rate was improved from 97.14% to 99.45%. Based on this result, it was observed that, up to a certain concentration, the incorporation of this nanocomposite into the PA layer could increase both the water flux and the salt rejection rate at the same time, meaning that under optimal concentration, the incorporation of GO/TiO_2 into the membrane did not cause defects in the TFN PA layer that would lead to a decrease in NaCl rejection, showing no trade-off effect between permeability and selectivity. A "trade-off" effect is characterized by a significant drop in salt rejection as permeability increases. This effect is very common and represents a major obstacle to the effective application of membranes [13].

In contrast to anionic salts, dyes are not only negatively charged but can also be positively charged or neutral. In a membrane functionalized with GO/TiO_2, Donnan exclusion is generally the main separation mechanism for negatively charged dyes. However, for neutral and positively charged dyes, size exclusion plays a vital role because although small molecules with dimensions much less than the interlayer spacing of the membrane can skip through, the large species might be blocked [38]. Figure 4 shows a schematic illustration of the proposed separation mechanism for neutral, negative charged, and positively charged molecules in a membrane functionalized with GO/TiO_2. In addition to Donnan exclusion and size exclusion, the overall membrane performance regarding dye rejection may also depend on the ability of GO to absorb dyes.

In a study by Ye et al. [59], researchers synthesized a

Table 2 Comparison in the impact of GO/TiO_2 on permeation flux and NaCl rejection for NF and RO membranes [19,66,70]

Membrane	Pressure/MPa	c(NaCl)/(mg·mL^{-1})	Permeation flux/(L·m^{-2}·h^{-1}·MPa^{-1})	NaCl rejection/%	Ref.
NF pristine membrane	0.01	2	40.5	81	[66]
NF membrane with eight layers of GO/TiO_2	0.01	2	62.3	97	[66]
RO pristine membrane	1.5	1	20.31	95.1	[70]
RO membrane with six layers of GO/TiO_2	1.5	1	23.6	96.3	[70]
RO pristine membrane	1.5	2	34.3	97.4	[19]
RO membrane with one layer of rGO/TiO_2	1.5	2	51.3	99.45	[19]

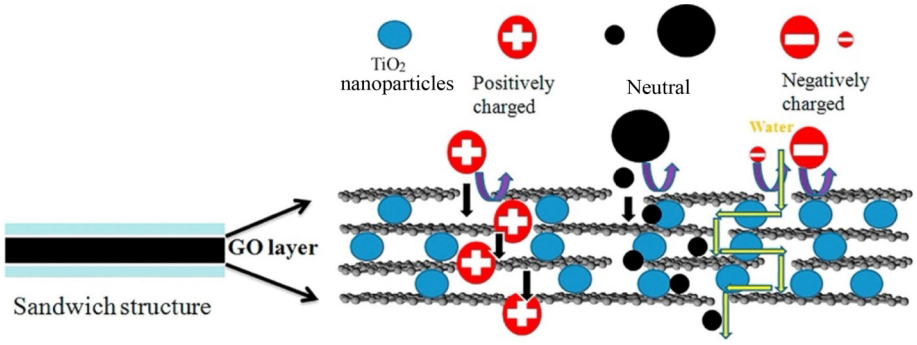

Fig. 4 Schematic illustration of the proposed separation mechanism for charged solutes (electrostatic repulsion and physical size sieving) and/or neutral molecules (physical size sieving). Reproduced from Ref. [38] with permission of Elsevier.

nanocomposite of GO nanosheets and TiO_2 nanorods. The high-performance membranes were prepared through vacuum filtration with varying concentrations of GO/TiO_2 nanocomposites onto the membrane surface. In NF tests, the rejection rates for negatively charged dyes such as Evans blue (EB) and methyl blue (MB) were more than 90%, significantly higher than that for the positively charged dye, methyl orange (MO), which was below 20%. The high rejection for negatively charged dyes was attributed to the electrostatic repulsion since the surface of the membranes with GO/TiO_2 nanocomposite incorporated is negatively charged, while size exclusion could be the main separation effect for MO. The results obtained with the membrane functionalized with GO/TiO_2 nanocomposite are analogous to the study of Yang et al. [57], which showed that after incorporating GO and graphitic carbon nitride nanomaterials ($GO/g\text{-}C_3N_4$), both negatively charged, the membrane had a higher removal rate for negatively charged dyes and a lower removal rate for positively charged dyes.

The dye separation mechanism in a membrane with GO/TiO_2 nanocomposites incorporated into its surface was also studied by Zhu et al. [71], who prepared a membrane with excellent structural stability, high dye rejection, and great permeability. Negatively charged solutions of chromium black T (CB), Congo red (CR), and brilliant blue R (BB) were used for the NF performance test, and all three dyes exhibited high rejection rates (> 95.4%). Due to the high rejection of negatively charged dyes, it is likely that electrostatic repulsion between the negative charges of dyes and the membrane surface was the dominant separation mechanism. However, it is also possible that the ability of GO to adsorb dyes play an important role in the separation process, since CB, a dye with lower molecular weight and shorter molecular length, shows a better rate of rejection than those of CR and BB. It is explained that this result could be caused by the formation of π–π bonds between GO and CB, thus CB would tend to be more easily adsorbed by GO, increasing its rejection rate.

Since fouling is one of the major challenges in membrane separation processes, the antifouling properties of GO/TiO_2 membranes have also been investigated. It was reported that the addition of GO/TiO_2 to NF and RO membranes increase the resistance to fouling of humic acid (HA), reactive red 48 (576 Da), reactive black 5 (992 Da), and bovine serum albumin (BSA) [19,43,72]. BSA is a protein that acts as an important foulant on the membrane surface via hydrophobic interactions, and it was suggested that BSA block membrane pores, resulting in a decline in flux [43]. In the study of Safarpour et al. [19], further to the formerly cited permeability and

selectivity test, RO membranes functionalized with GO/TiO_2 were also examined for their resistance to fouling, and the test was performed using 500 mg·L^{-1} of BSA solution as feed for the filtration system. The results showed that after 180 min of BSA filtration, the membrane without nanomaterials showed a higher loss of water flux decreasing to 49% of its initial flux, while membranes with 0.02 wt.% rGO/TiO_2 maintained approximately 75% of its initial flux value.

The GO/TiO_2 membranes also showed greater resistance to fouling in tests carried out with HA. In a research performed by Shao et al. [70], an RO membrane was synthesized with high performance and antifouling properties through incorporating GO/TiO_2 into a PA membrane using the layer-by-layer self-assembly method. The antifouling tests were carried out using a 5 mg·L^{-1} HA solution and based on its results was observed that compared to the pristine membrane, the membrane with GO/TiO_2 in PA layer showed a lower flux drop and a better flux recovery rate after rinsing. The better performance of GO/TiO_2 membranes in fouling resistance can be explained by the increase in membrane surface hydrophilicity and the decrease in surface roughness caused by the addition of GO/TiO_2 since the increasing hydrophilicity promotes the formation of an aqueous layer on the membrane surface, which should prevent fouling adsorption, and smoother surface makes it more difficult for foulant molecules to bind to the membrane surface [73–75]. The improvement in the fouling resistance of GO/TiO_2 membranes is also attributed to the increase in the negative charge on the membrane surface, as it makes it difficult for biofilms with a negative surface charge to attach to the membrane due to electrostatic repulsion [19].

4.1.2 Graphene oxide with zinc oxide (GO/ZnO)

The incorporation of GO/ZnO in membrane has been gaining interest because of traits consisting of excessive thermal and mechanical stability, anti-corrosive, and antimicrobial properties, and the fairly value in comparison to different metal oxide NPs, consisting of TiO_2 [76–77]. The study shows that the incorporation of GO/ZnO significantly increases the membrane water flux [78]. However, the most beneficial concentration of GO/ZnO depends on the membrane analyzed. In the work by Chung et al. [20], for example, the polysulfone (PSF) nanohybrid membrane was synthesized, and it was found that the concentration of 0.6 wt.% of GO/ZnO promoted the highest water flux (5.11 L·m^{-2}·h^{-1}·bar^{-1}), while for the RO PA membrane, the highest water flux (1.57 L·m^{-2}·h^{-1}·bar^{-1}) was achieved with 0.02 wt.% of GO/ZnO, as shown in the work of Rajakumaran et al. [78], since concentration higher than 0.02 wt.% caused a considerable decline in membrane permeability due to the pore blockage.

The improvement in membrane water flux after the incorporation of GO/ZnO is mainly attributed to the hydrophilic nature of these NPs. It is proposed that due to its high polarity, the addition of ZnO NPs presents a synergistic effect with GO resulting in the high hydrophilicity of the GO/ZnO film [20]. Furthermore, water adsorption on the surface of the membrane can be facilitated by the higher affinity between ZnO NPs and GO nanosheets that had a better interface for the dispersion of ZnO [19,78]. In addition to the concentration of GO/ZnO, the morphology of ZnO also influences the performance of the membrane. It was found that the incorporation of ZnO in spherical form resulted in superior performance compared to ZnO in both flower and rod forms. This result is attributed to the smaller size of the spherical shape, which inhibits GO nanosheets from stacking together [78].

Compared to that of TiO_2 NPs, ZnO NPs have a lower cost, which makes them very attractive for application in membranes. However, according to reports, the GO/ZnO membrane presents significantly a lower water flux than that of the TiO_2/GO membrane [19,78]. It was reported that after the incorporation of GO/ZnO in RO membranes at the optimum concentration of 0.02 wt.%, the water flux was 1.54 L·m^{-2}·h^{-1}·bar^{-1}, while the incorporation of GO/TiO_2 in RO membranes at 0.02 wt.% led to a water flux of 3.4 L·m^{-2}·h^{-1}·bar^{-1} [19,78]. The reason of the lower flux of the GO/ZnO membrane compared to that of the GO/TiO_2 membrane has not been analyzed in the literature yet. Thus, considering that water flux depends on hydrophilicity and particle size and aforementioned studies did not show either contact angles of the membranes or sizes of these hybrid nanomaterials, it is interesting that new studies compare the characteristics between GO/ZnO and GO/TiO_2 and their influence on membrane performance.

The influence of GO/ZnO on the contact angle of the PSF membrane was studied by Chung et al. [20] through incorporating nanohybrids on the PSF polymeric matrix. At the optimum concentration (2 wt.%), GO/ZnO decreases the membrane contact angle by 39.9% (from

65.9° of the bare membrane to 39.6° of the GO/ZnO membrane) [20]. Comparing to the study performed by Kusworo et al. [79], after the addition of GO/TiO_2 into the PSF polymeric matrix at the optimum concentration (1.5 wt.%), the reduction degree in contact angle was 32.6% (from 61.83° of the bare membrane to 41.7° of the GO/TiO_2 membrane) [79]. Therefore, considering that a smaller contact angle implies greater hydrophilicity [80], it is possible that the better water flux performance of GO/TiO_2 membranes compared to GO/ZnO membranes is not related to hydrophilicity. Instead, it is possible that a larger size of TiO_2 NPs result in a greater opening of the graphene sheets and consequently a greater water flux.

The contact angles of PSF membranes with GO/ZnO and with FeO/ZnO/GO incorporated on polymeric matrix were studied by Siddique et al. [81]. The results showed that the GO/ZnO membrane contact angle was 104° ± 3°, while for the GO/ZnO/FeO membrane, the contact angle was 87° ± 5°, indicating that the addition of FeO favors hydrophilicity. Thus, based on the results obtained by Siddique et al. [81] and considering that FeO has a lower cost than that of TiO_2, it is also proposed that new research further analyze the impact of adding GO/ZnO/FeO nanohybrids on the membrane performance, as well as comparing performances between the GO/TiO_2 membrane and the GO/ZnO/FeO membrane.

It has been reported that the incorporation of GO/ZnO nanocomposite into polymeric matrix of PSF membrane and onto PA layer of RO and NF membranes under optimal composition conditions could increase the percentage of rejection of several substances including salt [78], HA [20], and primary pollutants in petroleum refinery wastewater [79]. Regarding salt rejection, Rajakumaran et al. [78] found that the incorporation of GO/ZnO in the PA layer of RO membrane, with the same optimal concentration (0.02 wt.%) for water permeability, showed a rejection of 96.3%, lower than that of the membrane only containing GO (99.4%). However, percentage of the NaCl rejection above 95% is an acceptable value [13]. The reduction in salt rejection from membranes with GO/ZnO compared to membranes containing single GO could be a consequence of the increase in the spacing of GO interlayers caused by the presence of ZnO. The same behavior was observed in membranes incorporated with other GO-based nanohybrids, such as CNT/GO and CNC/GO, at the PA layer [82–83].

Rajakumaran et al. [78] also tested the impact of GO/ZnO on antifouling properties of the membrane. HA was used as foulant, and after 8 h of test the water flux of pristine TFN-RO has a drop of 41.1% from its initial water flux value, while in the membrane loaded with 0.02 wt.% of GO/ZnO (spherical Zn NPs), the water flux dropped only 13.7% from its initial value.

It is important to highlight that although the incorporation of GO/ZnO into the membrane enhance its antifouling properties, the filtration solution composition and the applied transmembrane pressure (TMP) could also influence the antifouling behaviors of membranes. This hypothesis was investigated through a study carried out by Siddique et al. [81], in which a bare PSF membrane and that with 1 wt.% of GO/ZnO into the polymer matrix were synthesized followed by the subjection to filtration fouling tests using a solution of As(III) (sodium (meta)arsenite, 90%) and a solution of As(V) (sodium arsenate dibasic heptahydrate) as contaminants with the TMP ranging from 2.5 to 6.25 bar (1 bar = 0.1 MPa). The result from the test with As(III) showed that for the membrane with GO/ZnO, increasing the pressure resulted in a higher percentage of the flux recovery rate (FRR). In contrast, in the test with As(V), it was observed that for the membrane containing GO/ZnO, the FRR decreased as the TMP increased. For the bare membrane, the FRR decreased by 51.3% when the pressure was increased by 1.25 bar. A comparison of filtration results indicated that the GO/ZnO membrane presented better antifouling performance towards the As(III) contaminant at the TMP of 6.25 bar than that towards As(V) at a lower TMP. These results suggest that the interaction between contaminants and GO/ZnO NPs, together with the TMP, plays a key role in influencing antifouling properties of the membrane.

The improved antifouling property of membranes with the incorporation of ZnO/GO is related to changes in roughness, hydrophilicity, and electrical charge of the membrane surface. It is suggested that the incorporation of GO/ZnO could reduce the surface roughness, which makes the adhesion of scale on the membrane surface difficult [78,84]. Also, because GO/ZnO is negatively charged, it suggested that it may promote electrostatic repulsion with negatively charged scales such as HA in the pH of brackish water [78]. The improvement of antifouling property of GO/ZnO membranes is also attributed to the hydrophilic nature of these nanomaterials, which likely results in the adsorption of organic pollutants within the membrane structure [20,77].

4.2 Graphene oxide with carbon-based nanomaterials

Like graphene, CNTs are allotropes of carbon. However, the structure of CNTs consists of one or more layers of carbon rolled into a long, hollow, and cylinder shape [18,70]. CNTs have properties that make them useful for various applications, including high strength, light weight, antifouling properties, self-cleaning properties, electrical capabilities, and adsorption capabilities. In addition, its hollow structure allows water molecules to be transported with low friction, making it highly advantageous for membrane applications [37,41]. Considering the excellent performance of GO and CNTs when individually incorporated into NF and RO membranes, it is very likely that GO/CNT nanohybrids can significantly improve the membrane performance. In recent years, several studies have been developed to understand the influence of GO/CNT on the membrane performance and make its application even more effective [85–86].

As already mentioned, the interlayer distance of GO is small. Therefore, it was suggested that the addition of CNTs could be an alternative solution to improving the interlayer distance of GO nanosheets, leading to the enhancement of the membrane permeability. Kang et al. [87] synthesized a composite membrane with sandwich morphology through layer-by-layer self-assembly incorporating GO nanohybrids with high and low contents of oxidized carbon nanotubes (OCNTs) onto a hydrolyzed polyacrylonitrile (hPAN) ultrafiltration membrane. Figure 5 shows a diagram of the GO/CNT membrane manufacturing process. According to water flux performance tests, incorporating GO/OCNTs with a high OCNT content significantly increased the permeability of the membrane, achieving a water flux of 28.53 $L \cdot m^{-2} \cdot h^{-1}$. On the other hand, GO/OCNT nanocomposites with a low distribution of OCNTs among GO nanosheets obtained low permeability, reaching a water flux of 14.98 $L \cdot m^{-2} \cdot h^{-1}$. It suggested that a low concentration of OCNTs among GO nanosheets could reduce the formation of interlayer support points, resulting in GO sheets experiencing various deformations under high pressures with the structural instability and decreased membrane water flux. In addition to increasing the space between GO interlayers, it is also suggested that GO/CNT nanocomposites can improve the membrane permeability through increasing the membrane surface hydrophilicity.

In a study conducted by Wei et al. [6], highly permeable and selective membranes were developed by incorporating graphene oxide with multi-walled carbon nanotube (GO/MWCNT) nanocomposites into the PA layer of the TFC membrane via IP using piperazine (PIP) and 1,3,5-benzenetricarbonyl trichloride (TMC) as monomers of polymerization solutions. The results showed that the water flux improved its initial value from approximately 41.7 to 55.6 $L \cdot m^{-2} \cdot h^{-1}$ after the incorporation of GO/MWCNT (6:3). The significant increase in permeability, surprisingly, did not compromise the salt rejection of the membranes with GO/MWCNT (6:3), which rejected 94% of Na_2SO_4, the same percentage of rejection of membranes containing only GO.

The hydrophilicity of membranes containing single GO was compared to that of membranes containing GO/CNT

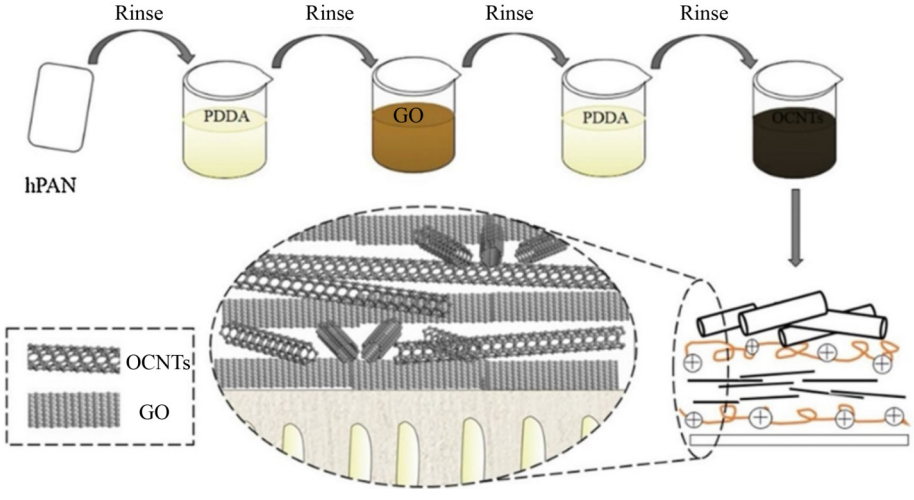

Fig. 5 Schematic illustration of the sandwich-like membrane formation via layer-by-layer self-assembly. Reproduced from Ref. [87] with permission of Elsevier.

nanohybrids through contact angle characterization. GO/CNT nanocomposite membranes were observed to have lower contact angles and, consequently, higher hydrophilicity than those of GO membranes. It has been suggested that the large amount of hydrophilic hydroxyl functional groups on the surface of MWCNTs may increase the attraction of more water molecules to the membrane surface, which improves the membrane permeation flux [88]. The above-mentioned effects can be compared with membranes containing functionalized hydroxyapatite (HAP) NP, which also showed improved hydrophilic properties of TFN-RO membranes [89]. Besides the hydrophilicity, the increase in the GO interlayer spacing caused by the presence of CNTs could create additional pathways leading water molecules to permeate more quickly [64]. In addition, the incorporation of MWCNTs may disrupt the diffusion rate of PIP, leading to the formation of a surface with relatively high roughness, which increases the permeate area of the membrane [90]. The combination of such three effects may have driven the improvement in water flux without the reduction of the salt rejection.

GO/MWCNT-incorporated membranes were found to be highly efficient in the removal of dyes. Previous studies have shown that although MWCNTs enlarge the GO nanochannels and allow the passage of more water, the nanochannels are still small enough to impede the passage of dye molecules, resulting in high dye rejection rates [82]. Furthermore, it is suggested that the separation mechanism can be influenced by the membrane surface charge [6]. In the study of Zeng et al. [88], for example, a high-efficiency NF membrane with 2D GO nanosheets and one-dimensional (1D) carboxylated multiwalled carbon nanotubes (MWCNTs-COOH) was synthesized and applied to treat organic wastewater. Membrane performance tests were performed using solutions containing methylene blue (MEB) as the positively charged dye, EB and MB as negatively charged dyes, and glucose and sucrose as neutrally charged molecules. The results showed that the MEB dye achieved a rejection of 99.7%, more than that for sucrose (97.3%) and that for EB (77%). It is important to highlight that the three-dimensional (3D) size of the negatively charged dye molecules used in the test is larger than that of the positively charged dye molecules, which means that the size exclusion effect was not the primary separation mechanism. Therefore, it is highly likely that the strong electrostatic interaction between the positively charged dye and the negatively charged membrane surface could have primarily driven positively charged dye retention. Although it is more common for membranes to repel molecules with the same charge via electrostatic repulsion, the high rejection of molecules with the same charge has been previously reported and is consistent with the report of Wang et al. [91], which suggests that electropositive dye molecules such as RhB and MB could be preferentially captured by GO/CNT nanocomposites effectively due to the π–π stacking and electrostatic interactions, resulting in the tight binding between dye molecules and GO-based nanosheets. However, for neutral molecules, size exclusion could be the main separation mechanism since the rejection of glucose (0.7 nm in diameter) was relatively lower than that of sucrose molecules (1.0 nm in diameter). In the study performed by Zheng and Mi [92], when a membrane functionalized with silica-crosslinked GO was synthesized, neutral organic molecules were much more efficiently rejected than negatively charged species in the test, and the high rejection of neutral molecules was attributed to the low partitioning and irreversible adsorption of neutral organic molecules into the silica-crosslinked GO membrane.

Considering the important function of CNTs between GO layers, Chen et al. [93] investigated the influence of CNT dispersion between GO nanosheets. A commercially available block copolymer (BCP) was used as a CNT dispersant. Thus, highly permeable, and selective membranes were synthesized with the incorporation of well-dispersed and poorly dispersed CNTs into rGO. rGO/CNTs were incorporated onto the membrane surface by the vacuum filtration method. When the membranes were subjected to dye removal tests, membranes with well-dispersed rGO/CNTs had a MO removal ratio of over 97.3% and water flux of 29.1 $L \cdot m^{-2} \cdot h^{-1}$, whereas membranes with poorly dispersed CNTs had a MO removal ratio of 61.2% and water flux of 27.1 $L \cdot m^{-2} \cdot h^{-1}$. The authors concluded that placing well-dispersed 1D CNTs within 2D graphene sheets allows the formation of a uniform network, which can provide many mass transfer channels through the continuous 3D nanostructure, resulting in high permeability and high dye separation performance. On the other hand, the poor dispersion of CNTs can harm the membrane performance due to the formation of defects on the membrane surface.

It is noted that GO/CNT nanocomposites have been widely used in the dye removal research. Table 3

[59,82–83,87–88,93] compares the water flux and dye rejection performance between NF membranes containing GO/CNT and NF membranes containing different nanomaterials. The results indicate that GO/CNT NFs have excellent dye rejection rates compared to other nanomaterials, achieving the highest MB rejection while maintaining good water flux.

It is important to highlight that the results presented in Table 3 are the most significant of each study, in which the concentrations of both nanomaterials incorporated in membranes and dyes in solutions are different in each study.

In the work of Han et al. [82], membranes with high performance of permeability and selectivity were synthesized by vacuum filtration of GO/CNT nanocomposites on a polyvinylidene fluoride (PVDF) support and its effect on the retention of magnesium salts ($MgSO_4$ and $MgCl_2$) and sodium salts (Na_2SO_4 and NaCl) was studied. According to the tests of water flux and ions rejection, membranes functionalized with GO/CNT have been discovered to have water permeability that completed more than two times the water permeability of single GO membrane. However, the incorporation of CNT results in a significant drop in salt rejection. In the NF membrane containing GO/CNT (8:1), the rejection rates of NaCl and Na_2SO_4 decreased from 59% and 95.1% to 51.4% and 80.9%, respectively, while the rejection rates of $MgSO_4$ and Mg_2Cl_2 decreased from 82.8% and 31.7% to 44.2% and 15.6%, respectively.

This drop is accentuated with the addition of a higher CNT content. With the addition of GO/CNT (8:5), the rejections of NaCl and Na_2SO_4 decreased to 39.6% and 71.2%, while those of $MgSO_4$ and $MgCl_2$ decreased to 25.1% and 9.5%, respectively. The retention order of different salt solutions obtained for GO/CNT membranes was Na_2SO_4 > NaCl > $MgSO_4$ > $MgCl_2$. Same behavior was obtained in the study by Chen et al. [93], where the salt rejection was also tested and the removal rates of Na_2SO_4 and NaCl were greater than that of $MgSO_4$ and $MgCl_2$. However, according to the literature, for a typical negatively charged NF membrane, the rejection rate for different inorganic salts is Na_2SO_4 > $MgSO_4$ > $MgCl_2$ > NaCl [6]. Based on the ions rejection results obtained by Han et al. [82] and Chen et al. [93], it is suggested that the presence of counterions that could bind part of the surface charge may have weakened the repulsion, resulting in low retention for the magnesium salt and high rejection of sodium salts [94]. Therefore, it is likely that the steric hindrance effect was the dominant mechanism for magnesium salt rejection, while the electrostatic repulsion effect appears to be the main separation mechanism for the sodium salts [82].

Table 3 Comparison of dye rejection and water flux values for NF membranes incorporated with various nanomaterials [59,82–83,87–88,93]

Nanomaterial	Dye rejection/%			Water flux/ ($L \cdot m^{-2} \cdot h^{-1}$)	Ref.
	MO	MB	RhB		
GO	–	98.4	99.2	70.6	[83]
	98.5	–	–	28.5	[82]
GO/TiO_2	14.5	90.7	–	420.2	[59]
GO/CNCs	–	96.2	98.4	81,7	[83]
rGO-CNTs	97.3	–	–	29.1	[93]
GO/OCNTs	–	99.3	–	21.7	[87]
GO/MWCNTs	98.0	–	–	48.1	[82]
GO/MWCNT-COOH	–	99.7	90.5	46.9	[88]

Several studies on the antifouling properties of GO/CNT membranes have been carried out and a significant increase in surface hydrophilicity and a decrease in surface roughness of the membranes were observed after the addition of GO/CNT nanocomposites [87,93]. In the work reported by Han et al. [82], for example, the contact angle decreases from ~63° of the membrane containing only GO to 53° of the membrane containing GO/CNT. Figure 6(a) shows the graph of water contact angles obtained by membranes with single GO and GO/CNT. Likewise, atomic force microscopy (AFM) analyses showed a drop in surface roughness, probably caused by a uniform self-assembly of GO/CNT nanocomposite on the membrane surface that did not generate agglomerates that could create damage on the surface of the membranes. Figures 6(b) and 6(c) show the AFM images and surface roughness analysis for membranes functionalized with GO and GO/CNT obtained from the study of Han et al. [82]. This improvement in hydrophilicity and roughness is certainly reflected in the results of antifouling property tests carried out with the HA solution, which revealed better performance obtained by membranes with GO/CNT than membranes with GO.

4.3 Graphene oxide with cellulose nanomaterials

4.3.1 Graphene oxide with cellulose nanocrystals (GO/CNCs)

CNCs are sustainable nanomaterials mainly obtained by

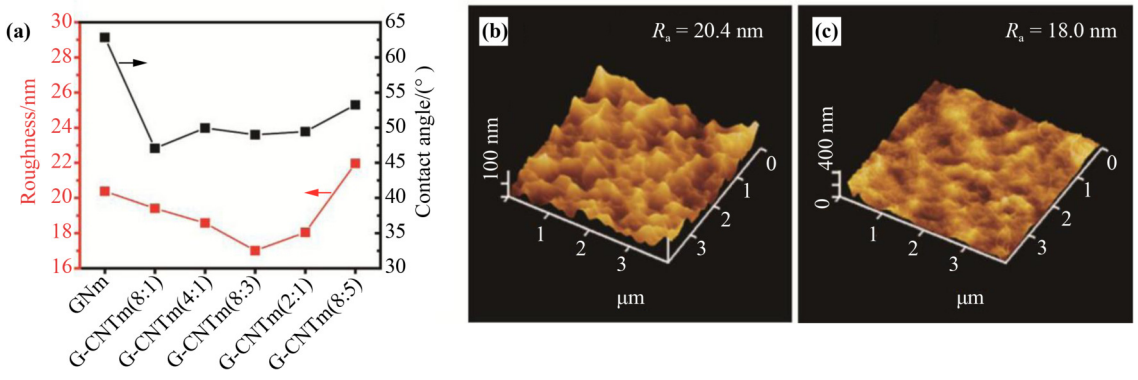

Fig. 6 (**a**) Surface roughness in terms of the average roughness (R_a) and the water contact angle for membranes with single GO (GNm) and GO/CNT (G-CNTms). Typical surface AFM images and surface roughness analyses for (**b**) GNm and (**c**) G-CNTm(2:1). Reproduced from Ref. [82] with permission of American Chemical Society.

acid hydrolysis of cellulose [95]. They have rod structures in various sizes and can be tens of nanometers in diameter and hundreds of nanometers in length [96]. CNCs are considered suitable candidates for application in water treatment membranes due to their excellent chemical and physical properties, such as high specific surface area (SSA), negative zeta potential, high Young's modulus, high hydrophilicity, antifouling ability, non-toxicity, biodegradability, and biocompatibility [96–97]. Previous studies have shown that GO/CNC nanohybrids have great potential for application in membranes [26,98]. When incorporated into NF and RO membranes, GO/CNC nanohybrids improved the membrane's hydrophilicity, permeability, and antifouling properties due to the excellent combined properties of both nanomaterials [99–101]. Figure 7 shows AFM images and schematic pictures of CNC and GO in single and hybrid configurations.

An investigation of effects of the incorporation of GO/CNCs into NF membranes was undertaken by Gao et al. [102]. To better compare the impact of single GO and GO/CNC nanocomposites in membrane permeability and selectivity of different antibiotics, GO and various concentrations of GO/CNC nanofillers were incorporated into a commercial PVDF substrate by the vacuum filtration process. In the salt water and pure water flux tests was observed that for membranes containing GO/CNC in different concentrations, the water permeability increased 2 to 4 times compared to the membrane control containing single GO, as represented in Fig. 8(a).

It was also observed that the membranes with higher concentrations of CNCs inside the GO/CNC nanohybrid

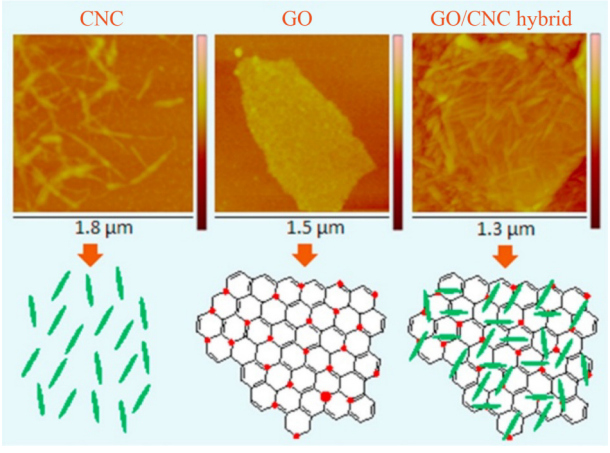

Fig. 7 Tapping mode AFM images and schematic illustrations of CNC, GO, and GO/CNC hybrid (GO:CNC-2:1) (red dots represent the oxygen-containing groups in GO). Reproduced from Ref. [99] with permission of Elsevier.

such as GC50 and GC65 (50 and 65 denotes the weight percentage of GO in the hybrid membrane) supplied better permeabilities with more water flux than those of commercial membranes (NF270 and NF90), which could indicate that the presence of CNCs increased the spacing between interlayers of GO nanosheets, facilitating water transport. In addition, the hydrophilic groups on CNCs could enhance the hydrophilicity of the membrane by enhancing its interaction with water [103]. The permeability may also have been increased due to the agglomeration of CNCs. In a study by Asempour et al. [42], when CNCs were incorporated into the membrane surface, they agglomerated, causing an increase in membrane surface roughness and the number of protuberances which might increase the effective surface area for permeation.

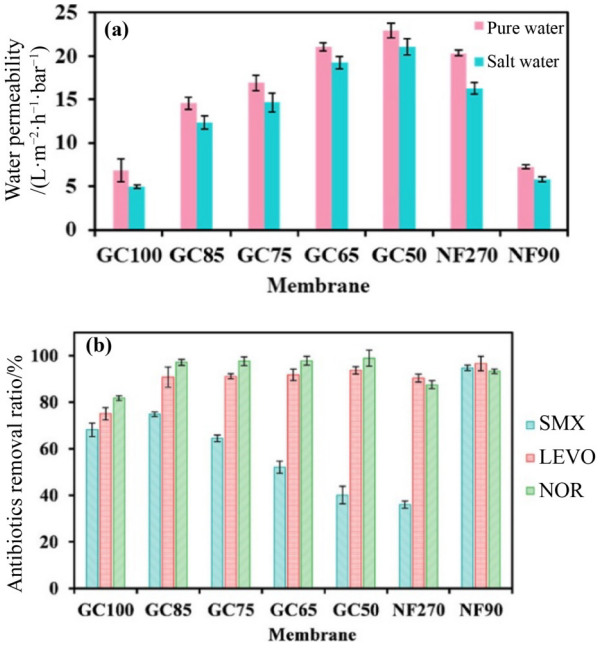

Fig. 8 (**a**) Pure water and salty water permeability values for membranes with different GO/CNC loadings. (**b**) Antibiotic separation performances of hybrid membranes including SMX, LEVO, and NOR. The obtained hybrid membranes were referred to as GCX (also known as GO/CNC-X), where X denotes the weight percentage of GO in the hybrid membrane, and both NF270 and NF90 refer to commercial membranes without nanomaterials. Reproduced from Ref. [102] with permission of American Chemical Society.

In the rejection tests, three antibiotics with different electrical potentials were tested: negatively charged sulfamethoxazole (SMX), slightly negatively charged levofloxacin (LEVO), and positively charged norfloxacin (NOR). The better rejection rates for each antibiotic were 74.8%, 90.9%, and 97.2%, respectively, obtained by the membrane GC85 (the GO/CNC nanocomposite with the GO concentration of 85%) as shown in Fig. 8(b). Zeta potential characterizations identified that the surface of the GO/CNC membrane was negatively charged, so it is possible that the rejection of negatively charged antibiotics was primarily driven by electrostatic repulsion [59]. On the other hand, NOR and LEVO (positively charged and slightly negatively charged, respectively) achieved higher rejection than the negatively charged antibiotic. It is suggested that LEVO and NOR were adsorbed by the membrane surface due to the electrostatic interactions which would nullify the membrane's role as a repellent. The same behavior was seen in the study of Zeng et al. [88], when GO/MWCNTs-COOH nanocomposites were incorporated into membranes and the results showed greater rejected rates of species positively charged than negatively charged. The antifouling characteristics of membranes generated by Gao et al. [102] were tested through the filtration of HA. Superior antifouling ability was exhibited by the membrane with GO/CNC compared to the membrane containing single GO. The increase in antifouling potential with the addition of CNCs was probably caused by the increase in surface hydrophilicity, which weakened the hydrophobic interaction, and the increase in negative surface charge increased the electrostatic repulsion of HA [70].

To ensure uniform dispersion of nanocomposites on the membrane surface, the nanocomposites should be regularly dispersed in water, as agglomeration of nanocomposites can increase surface roughness and make membranes more prone to fouling. GO contains highly hydrophilic functional groups, so it has good dispersibility in water. However, CNCs are prone to agglomeration. It is suggested that making changes on the surface of CNCs, such as the inclusion of carboxyl functional groups through carboxylation processes, can minimize the agglomeration tendency of this nanomaterial [104].

A study by Lyu et al. [83] evaluated the influence of nanohybrids of GO intercalated with different concentrations of carboxyl-modified nanocrystalline cellulose (CNCC) on the permeability and salt rejection performance of NF membranes. The GO/CNCC nanofillers were introduced onto the surface of a porous PVDF substrate via the vacuum filtration method. The results obtained from water flux performance tests showed that as the concentration of CCNCs in the GO/CNCC nanocomposite increased, the permeate water flux increased. The highest water flux was obtained when the amount of CNCC added in the film was 80% of GO content, reaching a flux of 12.74 $L \cdot m^{-2} \cdot h^{-1} \cdot bar^{-1}$, 66% greater than that of the membrane with single GO. However, it was also observed that the incorporation of GO/CNCC caused a decrease in the membrane selectivity. Comparing the results of ion rejections of the control membrane (with single GO incorporated) and the membrane with the GO/CNCC nanocomposite with 10% CNCC, drops were observed for the Na_2SO_4 rejection from 94.3% to 80.6%, the NaCl rejection from 52.5% to 47.5%, the $MgSO_4$ rejection from 83.9% to 75.4%, and the $MgCl_2$ rejection from 24.1% to 16.2%. In addition, it was also observed that this drop in salt rejection was accentuated by increasing the CNCC concentration. For example, for the GO/CNCC nanocomposite with 80% of CNCC, the drop of the salt rejection was even higher,

showing 19.8% for NaCl and 28.7% for Na_2SO_4. The same behavior was observed when the GO/CNCC membrane was tested for the separation of dyes. It was found that for dyes of Sunset Yellow (SY), MB, and RhB, the increase in the CNCC content of the GO/CNCC nanohybrid also reduced the rejection. However, this decrease was much smaller compared to the rejection of salts that still remained above 90% even with a concentration of 80% of CNCC.

Based on above-mentioned results, it is likely that both the improvement in water permeability and the drop in salt rejection presented by the GO/CNCC membrane were caused by the presence of CNCC in GO interlayers, which increased the spacing between GO nanosheets, promoting larger channels for the transport of water and solutes [38,69,82,102]. Furthermore, it is likely that this effect continued to be accentuated with increasing the concentration of CNCC in the nanohybrid [82]. It is important to highlight that the effect of GO/CNCC on rejection depends on the size of the species present in the feed solution. Therefore, increasing the spacing between GO layers due to the intercalation of CNCC results in a lower rejection rate when the size of NPs to be filtered is smaller than this spacing.

4.3.2 Graphene oxide with cellulose nanofibers (GO/CNFs)

Sustainable, non-toxic, and biocompatible CNFs are becoming even more essential as environment-friendly materials are increasingly sought in various industrial sectors [105]. The abundance of cellulose in nature, the low cost of synthesis, and the large-scale production make CNFs suitable for the membrane filtration application [106]. Moreover, CNFs have extraordinary properties, including a large surface-to-volume ratio, good flexibility, toughness, high strength, porosity, hydrophilicity, and high surface functionality due to the presence of functional groups [105,107–108]. Such aforementioned properties are highly desirable for application in membranes. In previous work, CNFs significantly improved the permeability and selectivity of RO membranes when compared to those of pristine membranes [109]. To take advantages of both CNFs and GO for the development of new hybrid nanomaterials used in the water purification process, researches on GO/CNF nanohybrids are progressing. The studies suggest that due to the strong interaction between CNFs and GO nanosheets through the formation of an extensive network of intermolecular hydrogen bonds, GO/CNF nanocomposites have synergistic effects [110–111].

Consequently, considering that GO and CNFs possess excellent individual properties that can be combined, the incorporation of GO/CNFs into NF and RO membranes is a promising option for developing high-performance and cost-effective membranes. In a research carried out by Mohammed et al. [112], highly permeable and selective NF membranes were synthesized by incorporating GO/CNF nanohybrids chemically crosslinked with glutaraldehyde (GA) into a nylon ultrafiltration membrane via the vacuum filtration method. Figure 9 shows a diagram of the GO/CNF NF membrane manufacturing process. In the permeability performance test, membranes with CNF/GO-20% (corresponding to the 20% GO concentration of the nanocomposite) showed better results, achieving a pure water flux of (13.9 ± 1.9) $L \cdot m^{-2} \cdot h^{-1} \cdot bar^{-1}$. However, in rejection tests for different organic dyes such as MO, RhB, BB, and rose Bengal (RB), the membrane CNF/GO-30% (corresponding to the 30% GO concentration of the nanocomposite) showed better results, achieving rejection rates for RB and BB above 90%, while the water flow rate was reduced to (8.8 ± 1.2) $L \cdot m^{-2} \cdot h^{-1} \cdot bar^{-1}$.

The results suggest that the higher GO concentration of GO/CNF nanohybrids, although with the increase of the membrane selectivity, may decrease the permeability. This behavior is likely caused by GO nanosheets that form a thicker selective layer, creating longer tortuous paths within membranes, hindering the transport of water and solutes [113]. However, higher concentrations of CNFs and lower concentrations of GO could probably present a larger water flux due to the high affinity of CNFs with water as well as the increased interlayer space of GO provided by the incorporation of CNFs that allows the transport of water and the passage of solutes, increasing the membrane's permeability and reducing the selectivity. The same behavior was observed in the work performed by Gao et al. [102] when GO/CNCs were incorporated into the membrane, as previously mentioned. According to the results of the selectivity experiments performed by Mohammed et al. [112], molecule size sieving and electrostatic repulsion were probably the dominant effects influencing the dye rejection. Presumably, size exclusion occurred because GO can act as molecular sieves to retain organic dye molecules larger than its nanogaps as reported by Joshi et al. [114], while the presence of carboxyl

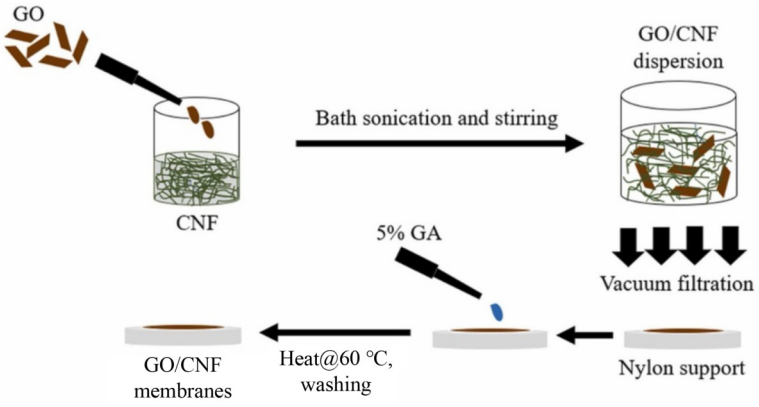

Fig. 9 Schematic illustration of fabrication steps for the GO/CNF NF membrane. Reproduced from Ref. [112] with permission of Elsevier.

groups in the GO/CNF stack led to the negatively charged membrane surface. As a result, dyes with larger molecular sizes and negatively charged dyes showed higher rejection rates [100,111,113].

4.4 Comparison of effects of incorporating different graphene oxide-based hybrid nanomaterials on membrane performances

As can be seen in the previous items, the results obtained in the literature show that GO-based nanohybrids significantly affect the performance of membranes mainly because after the incorporation of NPs into GO nanosheets, the interlayer distance of GO tends to increase, which can improve the membrane permeability. However, this effect tends to reduce the rejection rate of the substance to be filtered. Therefore, the main challenge in selecting NPs to be incorporated into GO is to prevent the increase in the distance between interlayers of GO nanosheets from reaching a level that could cause a significant decrease in the rejection rate.

Overall, the results reported in the literature indicate that NF and RO membranes functionalized with GO associated with TiO_2 NPs, CNTs, CNCs, and CNFs were able to significantly increase the permeability of water flux in the absence or presence of salt. Regarding dye rejection, it has been found that in membranes functionalized with GO/TiO_2, GO/CNTs, GO/CNCC, and GO/CNFs the rejection rate for different dyes was above 90%, which indicates acceptable performance [59,82–83,87–88,93]. On the other hand, about the salt rejection, GO/TiO_2 showed superior performance compared to GO/CNTs and GO/CNCs, since GO/TiO_2 simultaneously maintained increasing salt rejection and permeability [19,66]. In contrast, the other nanocomposites had decreasing rejection with increasing permeability [82–83,112]. The performance of GO/TiO_2 was possibly superior to other nanocomposites due to the size and shape of TiO_2 which increased the spacing between GO layers sufficiently to increase permeability without sacrificing selectivity. Thus, the size exclusion effect was minimized and the electrostatic repulsion between the membrane surface and the salt anions became predominant separation effect due to the increase of negative charges resulting from the incorporation of TiO_2. Regarding GO/CNF nanohybrids, more studies are needed to compare the performance of this nanohybrid with the others, and deeply analyze its effect on membrane water flux, selectivity, antifouling and chlorin resistance performance.

5 Future perspectives

GO-based hybrid nanomaterials have improved properties of several NF and RO membranes, but further advances are still needed. Most studies have shown that the trade-off effects could not be overcome even after incorporating GO-based nanohybrids into membranes. Therefore, the search for advanced GO-based hybrid nanomaterials that can simultaneously improve the membrane permeability and selectivity should continue. As wastewater treatment moves towards more ecofriendly options, researches in hybrid nanomaterials based on GO and biopolymeric nanomaterials, such as chitosan and CNFs, together with the green synthesis of GO applied to membrane for seawater and wastewater treatment should be better explored, as well as its effects in leaching out.

Considering the great demand for membranes used in desalination and the advantage that CNCs present over ceramic NPs from an economic point of view and environmental save, it is important to carry out studies to improve the salt rejection performance of CNCs. It is possible that to improve the performance of CNCs in terms of salt rejection, it could be feasible to reduce the size or thickness of these nanostructures, which could consequently mitigate the effect that their presence causes in increasing the spacing between GO layers. In addition, it has been suggested that reducing the agglomeration of CNCs can improve the salt rejection performance [42].

It has been found from Refs. [115–117] that nanocrystals obtained from cotton fibers, when incorporated into the Zn deposit, result in greater corrosion resistance compared to nanocrystals obtained from sisal fibers and soybean hulls. This effect is related to the lower agglomeration of nanocrystals obtained from cotton fibers. Therefore, these results indicate that the nature of the material from which the nanocrystal is obtained can affect the level of agglomeration. In work involving the incorporation of CNCC into GO, the nanocrystals consist of only cellulose, while the nanocrystals obtained from cotton fibers also contain hemicellulose. Therefore, it is interesting to evaluate the effect of incorporating CNCs obtained from cotton fibers into GO aiming to reduce the possibility of aggregation onto membrane surface.

It is known that membranes containing nanomaterials have not yet been commercialized. To improve the performance of NF and RO membranes for industrial-scale applications, several aspects should be considered in future researches:

1) Long term performance — After a long-term operation, the membrane performance may be reduced and require cleaning and maintenance. However, the long-term performance has not been investigated in most studies. Future researches should provide a more detailed assessment of long-term performance. During operation, a detailed maintenance and cleaning schedule is required.

2) Scale-up process design and cost-efficiency — The application of GO-based nanohybrids to industrial-scale membranes has not been investigated, as most studies have limited their studies to the laboratory scale. Therefore, future researches must be able to evaluate the fabrication methods and applications of these nanomaterials in profitable and large-scale membranes. However, effective implementation of technology at scale requires a thorough evaluation of the entire economic process.

3) Environmental impact — The environmental impact of nanofillers must be considered, as nanomaterials exposed on the membrane surface may be washed away and lead to secondary contamination. The effects of nanomaterials used in water treatment membranes require careful research, mainly focusing on long-term and short-term environmental damage and possible toxicity to humans and animals. As nanomaterials have highly reactive structures, they can interact with other pollutants and produce structures with low or high toxicity [13]. Therefore, it is very important to assess the impact of nanomaterials from filtered water to post-use disposal.

6 Conclusions

We comprehensively reviewed the research progress of embedding GO-based nanohybrids in NF and RO membranes for water purification and desalination and focused on the mechanism of hybrid NPs to enhance the water permeance, ion and dye rejection of membranes, and anti-fouling resistance. GO-based nanohybrids integrated into membranes represent a major advance in NF and RO processes. In studies using membranes containing single GO, difficulty was noted in improving permeability. However, most of GO-based hybrid nanomaterials showed a significant reduction in nanocomposite agglomeration and surface defects, resulting in improved membrane permeability, selectivity, and resistance to fouling. Essentially, the improvement in aforementioned properties is attributed to the compositions and structures of two nanostructures, including the presence of hydrophilic functional groups and the good dispersion of the nanomaterial within GO. Furthermore, one of the main reasons for the increased permeability of membranes functionalized with GO-based nanohybrids is that the nanomaterials dispersed in GO nanosheets may increase the interlayer space of GO, creating a larger pathway for water transport. It is also possible to conclude that the nanomaterials bring a negative charge to the membrane surface, which contributes to the improvement in selectivity performances and antifouling properties of membranes.

Declaration of competing interests The authors declare no conflict of interest in the content of this work.

Acknowledgements These authors would like to acknowledge the financial support of COORDENAÇÃO DE APERFEIÇOAMENTO DE PESSOAL DE NÍVEL SUPERIOR (CAPES).

References

[1] Aberilla J M, Gallego-Schmid A, Stamford L, et al. Environmental assessment of domestic water supply options for remote communities. Water Research, 2020, 175: 115687

[2] DesalData. The IDA Water Security Handbook 2000–2021. Oxford, UK: Media Analytics Ltd., 2020

[3] Karki S, Gohain M B, Yadav D, et al. Building rapid water transport channels within thin-film nanocomposite membranes based on 2D mesoporous nanosheets. Desalination, 2023, 547: 116222

[4] Yang F, Cui F, Yuan Y D, et al. Mechanistic insights into the role of nanoparticles towards the enhanced performance of thin-film nanocomposite membranes. Journal of Membrane Science Letters, 2023, 3(1): 100046

[5] Qin X M, Qin X Y, Xu X R, et al. The membrane-based desalination: focus on MOFs and COFs. Desalination, 2023, 557: 116598

[6] Wei X, Cao S, Hu J, et al. Graphene oxide/multi-walled carbon nanotubes nanocompsite polyamide nanofiltration membrane for dyeing-printing wastewater treatment. Polymers for Advanced Technologies, 2021, 32(2): 690−702

[7] Huo H Q, Mi Y F, Yang X, et al. Polyamide thin film nanocomposite membranes with *in-situ* integration of multiple functional nanoparticles for high performance reverse osmosis. Journal of Membrane Science, 2023, 669: 121311

[8] Bai L, Liu Y, Ding A, et al. Fabrication and characterization of thin-film composite (TFC) nanofiltration membranes incorporated with cellulose nanocrystals (CNCs) for enhanced desalination performance and dye removal. Chemical Engineering Journal, 2019, 358: 1519−1528

[9] An M, Gutierrez L, D'Haese A, et al. *In-situ* modification of nanofiltration and reverse osmosis membranes for organic micropollutants and salts removal: a review. Desalination, 2023, 565: 116861

[10] Shams A, Mirbagheri S A, Jahani Y. The synergistic effect of graphene oxide and POSS in mixed matrix membranes for desalination. Desalination, 2019, 472: 114131

[11] Chantaso M, Chaiyong K, Meesupthong R, et al. Sugarcane leave-derived cellulose nanocrystal/graphene oxide filter membrane for efficient removal of particulate matter. International Journal of Biological Macromolecules, 2023, 234: 123676

[12] Al-Gamal A Q, Satria M, Alghunaimi F I, et al. Synthesis of thin-film nanocomposite membranes using functionalized silica nanoparticles for water desalination with drastically improved properties. Reactive & Functional Polymers, 2022, 181: 105433

[13] Saleem H, Zaidi S J. Nanoparticles in reverse osmosis membranes for desalination: a state of the art review. Desalination, 2020, 475: 114171

[14] Tong Y, Wei Y, Zhang H, et al. Fabrication of polyamide thin film nanocomposite membranes with enhanced desalination performance modified by silica nanoparticles formed *in-situ* polymerization of tetramethoxysilane. Journal of Environmental Chemical Engineering, 2023, 11(2): 109415

[15] El-Aassar A H M A. Improvement of reverse osmosis performance of polyamide thin-film composite membranes using TiO_2 nanoparticles. Desalination and Water Treatment, 2015, 55(11): 2939−2950

[16] Ben-Sasson M, Lu X, Bar-Zeev E, et al. *In situ* formation of silver nanoparticles on thin-film composite reverse osmosis membranes for biofouling mitigation. Water Research, 2014, 62: 260−270

[17] Yin J, Zhu G, Deng B. Graphene oxide (GO) enhanced polyamide (PA) thin-film nanocomposite (TFN) membrane for water purification. Desalination, 2016, 379: 93−101

[18] Teow Y H, Mohammad A W. New generation nanomaterials for water desalination: a review. Desalination, 2019, 451: 2−17

[19] Safarpour M, Khataee A, Vatanpour V. Thin film nanocomposite reverse osmosis membrane modified by reduced graphene oxide/TiO_2 with improved desalination performance. Journal of Membrane Science, 2015, 489: 43−54

[20] Chung Y T, Mahmoudi E, Mohammad A W, et al. Development of polysulfone-nanohybrid membranes using ZnO–GO composite for enhanced antifouling and antibacterial control. Desalination, 2017, 402: 123−132

[21] Bagheripour E, Moghadassi A R, Hosseini S M, et al. Novel composite graphene oxide/chitosan nanoplates incorporated into PES based nanofiltration membrane: chromium removal and antifouling enhancement. Journal of Industrial and Engineering Chemistry, 2018, 62: 311−320

[22] Huang H H, Joshi R K, De Silva K K H, et al. Fabrication of reduced graphene oxide membranes for water desalination. Journal of Membrane Science, 2019, 572: 12−19

[23] de Oliveira C P M, Farah I F, Koch K, et al. TiO_2–graphene oxide nanocomposite membranes: a review. Separation and Purification Technology, 2022, 280: 119836

[24] Thakre K G, Barai D P, Bhanvase B A. A review of graphene–TiO_2 and graphene–ZnO nanocomposite photocatalysts for wastewater treatment. Water Environment Research, 2021, 93(11): 2414−2460

[25] Alnajjar H, Tabatabai A, Alpatova A, et al. Organic fouling control in reverse osmosis (RO) by effective membrane cleaning using saturated CO_2 solution. Separation and Purification Technology, 2021, 264: 118410

[26] Bai L, Ding A, Li G, et al. Application of cellulose nanocrystals in water treatment membranes: a review. Chemosphere, 2022, 308: 136426

[27] Abuwatfa W H, AlSawaftah N, Darwish N, et al. A review on membrane fouling prediction using artificial neural networks (ANNs). Membranes, 2023, 13(7): 685

[28] Yang G, Sun M, Wang C, et al. Dual regulation of graphene oxide membrane by crosslinker and hydrophilic promoter for dye separation. Microporous and Mesoporous Materials, 2023, 360: 112718

[29] Guan D, Hu Z, Xie P, et al. Osmotic cleaning to control inorganic fouling of nanofiltration membrane for seawater desalination. Journal of Environmental Chemical Engineering, 2023, 11(5): 110551

[30] Wang J, Xu R, Yang F, et al. Probing influences of support layer on the morphology of polyamide selective layer of thin film composite membrane. Journal of Membrane Science, 2018, 556: 374−383

[31] Ahmed M A, Amin S, Mohamed A A. Fouling in reverse osmosis membranes: monitoring, characterization, mitigation strategies and future directions. Heliyon, 2023, 9(4): e14908

[32] Mahlangu O T, Nthunya L N, Motsa M M, et al. Fouling of high pressure-driven NF and RO membranes in desalination processes: mechanisms and implications on salt rejection. Chemical Engineering Research & Design, 2023, 199: 268−295

[33] Jhaveri J H, Murthy Z V P. A comprehensive review on anti-fouling nanocomposite membranes for pressure driven membrane separation processes. Desalination, 2016, 379: 137−154

[34] Ng Z C, Lau W J, Matsuura T, et al. Thin film nanocomposite RO membranes: review on fabrication techniques and impacts of nanofiller characteristics on membrane properties. Chemical Engineering Research & Design, 2021, 165: 81−105

[35] Amiri S, Vatanpour V, He T. Antifouling thin-film nanocomposite NF membrane with polyvinyl alcohol–sodium alginate–graphene oxide nanocomposite hydrogel coated layer for As(III) removal. Chemosphere, 2023, 322: 138159

[36] Wang S Y, Gonzales R R, Zhang P, et al. Surface charge control of poly(methyl methacrylate-co-dimethyl aminoethyl methacrylate)-based membrane for improved fouling resistance. Separation and Purification Technology, 2021, 279: 119778

[37] Azelee I W, Goh P S, Lau W J, et al. Enhanced desalination of polyamide thin film nanocomposite incorporated with acid treated multiwalled carbon nanotube–titania nanotube hybrid. Desalination, 2017, 409: 163−170

[38] Chen L, Li N, Wen Z, et al. Graphene oxide based membrane intercalated by nanoparticles for high performance nanofiltration application. Chemical Engineering Journal, 2018, 347: 12−18

[39] Chae H R, Lee J, Lee C H, et al. Graphene oxide-embedded thin-film composite reverse osmosis membrane with high flux, anti-biofouling, and chlorine resistance. Journal of Membrane Science, 2015, 483: 128−135

[40] Vaishnavi P S V, Kar S, Adak A K, et al. Surface modification of thin film composite nanofiltration membrane with graphene oxide by varying amine linkers: synthesis, characterization, and applications. Journal of Membrane Science, 2023, 687: 122021

[41] Long L, Wu C, Yang Z, et al. Carbon nanotube interlayer enhances water permeance and antifouling performance of nanofiltration membranes: mechanisms and experimental evidence. Environmental Science & Technology, 2022, 56(4): 2656−2664

[42] Asempour F, Emadzadeh D, Matsuura T, et al. Synthesis and characterization of novel cellulose nanocrystals-based thin film nanocomposite membranes for reverse osmosis applications. Desalination, 2018, 439: 179−187

[43] Wang J, Wang Y, Zhu J, et al. Construction of TiO_2@graphene oxide incorporated antifouling nanofiltration membrane with elevated filtration performance. Journal of Membrane Science, 2017, 533: 279−288

[44] Johnson D J, Hilal N. Can graphene and graphene oxide materials revolutionise desalination processes? Desalination, 2021, 500: 114852

[45] Zankana M M, Al-dalawy S M, Barzinjy A A. Synthesis and characterization of bio-nanocomposites: functionalization of graphene oxide with a biocompatible amino acid. Hybrid Advances, 2023, 3: 100070

[46] Kausar A. Conjugated polymer/graphene oxide nanocomposites — state-of-the-art. Journal of Composites Science, 2021, 5(11): 292

[47] Farjadian F, Abbaspour S, Sadatlu M A A, et al. Recent developments in graphene and graphene oxide: properties, synthesis, and modifications: a review. ChemistrySelect, 2020, 5(33): 10200−10219

[48] Hummers W S, Offeman R E. Preparation of graphitic oxide. Journal of the American Chemical Society, 1958, 80(6): 1339

[49] Wu W, Shi Y, Liu G, et al. Recent development of graphene oxide based forward osmosis membrane for water treatment: a critical review. Desalination, 2020, 491: 114452

[50] Lerf A, He H Y, Forster M, et al. Structure of graphite oxide revisited. The Journal of Physical Chemistry B, 1998, 102(23): 4477−4482

[51] He H Y, Klinowski J, Forster M, et al. A new structural model for graphite oxide. Chemical Physics Letters, 1998, 287(1−2): 53−56

[52] Yu W, Sisi L, Haiyan Y, et al. Progress in the functional modification of graphene/graphene oxide: a review. RSC Advances, 2020, 10(26): 15328−15345

[53] Liu Q, Xu G R. Graphene oxide (GO) as functional material in tailoring polyamide thin film composite (PA-TFC) reverse osmosis (RO) membranes. Desalination, 2016, 394: 162−175

[54] Foller T, Wen X, Khine Y Y, et al. Removal of chlorine and monochloramine from tap water using graphene oxide membranes. Journal of Membrane Science, 2023, 686: 122022

[55] Zhao W, Liu H, Meng N, et al. Graphene oxide incorporated thin film nanocomposite membrane at low concentration monomers. Journal of Membrane Science, 2018, 565: 380−389

[56] Oikawa M, Takeuchi H, Chikyu D, et al. Insight into the role of ionicity in the desalination and separation of a graphene oxide membrane. Desalination, 2023, 552: 116433

[57] Yang L, Jia F, Juan Z, et al. High-permeable graphene oxide/graphitic carbon nitride composite nanofiltration membrane for selective separation of dye and desalination. Journal of Environmental Chemical Engineering, 2023, 11(2): 109306

[58] Yan X, Huo L, Ma C, et al. Layer-by-layer assembly of graphene oxide–TiO_2 membranes for enhanced photocatalytic and self-cleaning performance. Process Safety and Environmental Protection, 2019, 130: 257−264

[59] Ye Z, Yang L, Wang Y, et al. Graphene oxide membranes intercalated with titanium dioxide nanorods for fast infiltration and dye separation. FlatChem, 2023, 38: 100488

[60] Zhang H, Li X, Xu T. Two-dimensional graphene oxide nanochannel membranes for ionic separation. Current Opinion in Chemical Engineering, 2023, 39: 100899

[61] Faria A F, Liu C, Xie M, et al. Thin-film composite forward osmosis membranes functionalized with graphene oxide–silver nanocomposites for biofouling control. Journal of Membrane Science, 2017, 525: 146−156

[62] Al Mayyahi A. Thin-film composite (TFC) membrane modified by hybrid ZnO–graphene nanoparticles (ZnO–Gr NPs) for water desalination. Journal of Environmental Chemical Engineering, 2018, 6(1): 1109−1117

[63] Abadikhah H, Kalali E N, Behzadi S, et al. High flux thin film nanocomposite membrane incorporated with functionalized TiO_2@reduced graphene oxide nanohybrids for organic solvent nanofiltration. Chemical Engineering Science, 2019, 204: 99−109

[64] Ali F A A, Alam J, Shukla A K, et al. Graphene oxide–silver nanosheet-incorporated polyamide thin-film composite membranes for antifouling and antibacterial action against *Escherichia coli* and bovine serum albumin. Journal of Industrial and Engineering Chemistry, 2019, 80: 227−238

[65] Dong L, Li M, Zhang S, et al. NH_2-Fe_3O_4-regulated graphene oxide membranes with well-defined laminar nanochannels for desalination of dye solutions. Desalination, 2020, 476: 114227

[66] Al-Gamal A Q, Falath W S, Saleh T A. Enhanced efficiency of polyamide membranes by incorporating TiO_2–graphene oxide for water purification. Journal of Molecular Liquids, 2021, 323: 114922

[67] Yang T, Liu Y, Xia G, et al. Degradation of formaldehyde and methylene blue using wood-templated biomimetic TiO_2. Journal of Cleaner Production, 2021, 329: 129726

[68] Emadzadeh D, Lau W J, Matsuura T, et al. Synthesis and characterization of thin film nanocomposite forward osmosis membrane with hydrophilic nanocomposite support to reduce internal concentration polarization. Journal of Membrane Science, 2014, 449: 74−85

[69] Qian X, Wang X, Gao X, et al. Effects of GO@CS core–shell nanomaterials loading positions on the properties of thin film nanocomposite membranes. Journal of Membrane Science, 2021, 624: 119102

[70] Shao F, Xu C, Ji W, et al. Layer-by-layer self-assembly TiO_2 and graphene oxide on polyamide reverse osmosis membranes with improved membrane durability. Desalination, 2017, 423: 21−29

[71] Zhu L, Wu M, Van der Bruggen B, et al. Effect of TiO_2 content on the properties of polysulfone nanofiltration membranes modified with a layer of TiO_2–graphene oxide. Separation and Purification Technology, 2020, 242: 116770

[72] Liu Y, Yu Z, Peng Y, et al. A novel photocatalytic self-cleaning TiO_2 nanorods inserted graphene oxide-based nanofiltration membrane. Chemical Physics Letters, 2020, 749: 137424

[73] Zhang R, Li Y, Su Y, et al. Engineering amphiphilic nanofiltration membrane surfaces with a multi-defense mechanism for improved antifouling performances. Journal of Materials Chemistry A: Materials for Energy and Sustainability, 2016, 4(20): 7892−7902

[74] Tang Y J, Xu Z L, Xue S M, et al. A chlorine-tolerant nanofiltration membrane prepared by the mixed diamine monomers of PIP and BHTTM. Journal of Membrane Science, 2016, 498: 374−384

[75] Zhu J, Qin L, Uliana A, et al. Elevated performance of thin film nanocomposite membranes enabled by modified hydrophilic MOFs for nanofiltration. ACS Applied Materials & Interfaces, 2017, 9(2): 1975−1986

[76] Vaseem M, Umar A, Hahn Y B. ZnO nanoparticles: growth, properties, and applications. In: Umar A, ed. Metal Oxide

Nanostructures and Their Applications. Stevenson Ranch, CA: American Scientific Publishers, 2010

[77] Balta S, Sotto A, Luis P, et al. A new outlook on membrane enhancement with nanoparticles: the alternative of ZnO. Journal of Membrane Science, 2012, 389: 155−161

[78] Rajakumaran R, Boddu V, Kumar M, et al. Effect of ZnO morphology on GO–ZnO modified polyamide reverse osmosis membranes for desalination. Desalination, 2019, 467: 245−256

[79] Kusworo T D, Dalanta F, Aryanti N, et al. Intensifying separation and antifouling performance of PSf membrane incorporated by GO and ZnO nanoparticles for petroleum refinery wastewater treatment. Journal of Water Process Engineering, 2021, 41: 102030

[80] Mahmoudi E, Ng L Y, Ba-Abbad M M, et al. Novel nanohybrid polysulfone membrane embedded with silver nanoparticles on graphene oxide nanoplates. Chemical Engineering Journal, 2015, 277: 1−10

[81] Siddique T, Gangadoo S, Pham D Q, et al. Antifouling and antimicrobial study of nanostructured mixed-matrix membranes for arsenic filtration. Nanomaterials, 2023, 13(4): 738

[82] Han Y, Jiang Y, Gao C. High-flux graphene oxide nanofiltration membrane intercalated by carbon nanotubes. ACS Applied Materials & Interfaces, 2015, 7(15): 8147−8155

[83] Lyu Y, Zhang Q, Wang Z, et al. A graphene oxide nanofiltration membrane intercalated with cellulose nano-crystals. BioResources, 2018, 13(4): 9116−9131

[84] Lawler J. Incorporation of graphene-related carbon nanosheets in membrane fabrication for water treatment: a review. Membranes, 2016, 6(4): 57

[85] Chae J, Cheng H, Lim T, et al. A study on the effects of the addition of graphene oxide and multi-walled carbon nanotubes for surface modification on polyvinylidene fluoride membranes. Materials Letters, 2022, 309: 131311

[86] Han F, Mao J, Liu S. Preparation of reduced graphene oxide–carbon nanotubes membranes for conductive heating membrane distillation treatment of humic acid. Separation and Purification Technology, 2022, 302: 122181

[87] Kang H, Shi J, Liu L, et al. Sandwich morphology and superior dye-removal performances for nanofiltration membranes self-assemblied via graphene oxide and carbon nanotubes. Applied Surface Science, 2018, 428: 990−999

[88] Zeng W J, Li C, Feng Y, et al. Carboxylated multi-walled carbon nanotubes (MWCNTs-COOH)-intercalated graphene oxide membranes for highly efficient treatment of organic wastewater. Journal of Water Process Engineering, 2021, 40: 101901

[89] Ohland A L, Salim V M M, Borges C P. Nanocomposite membranes for osmotic processes: Incorporation of functionalized hydroxyapatite in porous substrate and in selective layer. Desalination, 2019, 463: 23−31

[90] Xue S M, Xu Z L, Tang Y J, et al. Polypiperazine-amide nanofiltration membrane modified by different functionalized multiwalled carbon nanotubes (MWCNTs). ACS Applied Materials & Interfaces, 2016, 8(29): 19135−19144

[91] Wang C Y, Zeng W J, Jiang T T, et al. Incorporating attapulgite nanorods into graphene oxide nanofiltration membranes for efficient dyes wastewater treatment. Separation and Purification Technology, 2019, 214: 21−30

[92] Zheng S, Mi B. Emerging investigators series: silica-crosslinked graphene oxide membrane and its unique capability in removing neutral organic molecules from water. Environmental Science: Water Research & Technology, 2016, 2(4): 717−725

[93] Chen X, Qiu M, Ding H, et al. A reduced graphene oxide nanofiltration membrane intercalated by well-dispersed carbon nanotubes for drinking water purification. Nanoscale, 2016, 8(10): 5696−5705

[94] Soomro F, Memon F H, Khan M A, et al. Ultrathin graphene oxide-based nanocomposite membranes for water purification. Membranes, 2023, 13(1): 64

[95] Vanderfleet O M, D'Acierno F, Isogai A, et al. Effects of surface chemistry and counterion selection on the thermal behavior of carboxylated cellulose nanocrystals. Chemistry of Materials, 2022, 34(18): 8248−8261

[96] Abedi F, Emadzadeh D, Dubé M A, et al. Modifying cellulose nanocrystal dispersibility to address the permeability/selectivity trade-off of thin-film nanocomposite reverse osmosis membranes. Desalination, 2022, 538: 115900

[97] Rajendran N, Runge T, Bergman R D, et al. Techno-economic analysis and life cycle assessment of cellulose nanocrystals production from wood pulp. Bioresource Technology, 2023, 377: 128955

[98] Lv J, Zhang G, Zhang H, et al. Graphene oxide–cellulose nanocrystal (GO–CNC) composite functionalized PVDF membrane with improved antifouling performance in MBR: behavior and mechanism. Chemical Engineering Journal, 2018, 352: 765−773

[99] El Miri N, El Achaby M, Fihri A, et al. Synergistic effect of cellulose nanocrystals/graphene oxide nanosheets as functional hybrid nanofiller for enhancing properties of PVA nanocomposites. Carbohydrate Polymers, 2016, 137: 239−248

[100] Fang Q, Zhou X, Deng W, et al. Freestanding bacterial cellulose–graphene oxide composite membranes with high mechanical strength for selective ion permeation. Scientific Reports, 2016, 6(1): 33185

[101] Ding Z, Tang Y, Zhu P. Reduced graphene oxide/cellulose

nanocrystal composite films with high specific capacitance and tensile strength. International Journal of Biological Macromolecules, 2022, 200: 574−582

[102] Gao H, Wang Y, Afolabi M A, et al. Incorporation of cellulose nanocrystals into graphene oxide membranes for efficient antibiotic removal at high nutrient recovery. ACS Applied Materials & Interfaces, 2021, 13(12): 14102−14111

[103] Trache D, Thakur V K, Boukherroub R. Cellulose nanocrystals/graphene hybrids — a promising new class of materials for advanced applications. Nanomaterials, 2020, 10(8): 1523

[104] Lam E, Hemraz U D. Preparation and surface functionalization of carboxylated cellulose nanocrystals. Nanomaterials, 2021, 11(7): 1641

[105] Das R, Lindström T, Sharma P R, et al. Nanocellulose for sustainable water purification. Chemical Reviews, 2022, 122(9): 8936−9031

[106] Azimi B, Sepahvand S, Ismaeilimoghadam S, et al. Application of cellulose-based materials as water purification filters; a state-of-the-art review. Journal of Polymers and the Environment, 2024, 32(1): 345−366

[107] Lamm M E, Li K, Qian J, et al. Recent advances in functional materials through cellulose nanofiber templating. Advanced Materials, 2021, 33(12): 2005538

[108] Zhang B, Duan W, Wang Y, et al. Recent advances of cellulose nanofiber-based materials in cell culture: from population to single-cell. TRAC-Trends in Analytical Chemistry, 2023, 166: 117159

[109] Liu S, Low Z X, Hegab H M, et al. Enhancement of desalination performance of thin-film nanocomposite membrane by cellulose nanofibers. Journal of Membrane Science, 2019, 592: 117363

[110] Zhu C, Liu P, Mathew A P. Self-assembled TEMPO cellulose nanofibers: graphene oxide-based biohybrids for water purification. ACS Applied Materials & Interfaces, 2017, 9(24): 21048−21058

[111] Liu P, Zhu C, Mathew A P. Mechanically robust high flux graphene oxide–nanocellulose membranes for dye removal from water. Journal of Hazardous Materials, 2019, 371: 484−493

[112] Mohammed S, Hegab H M, Ou R. Nanofiltration performance of glutaraldehyde crosslinked graphene oxide–cellulose nanofiber membrane. Chemical Engineering Research & Design, 2022, 183: 1−12

[113] Mohammed S, Hegab H M, Ou R, et al. Effect of oxygen plasma treatment on the nanofiltration performance of reduced graphene oxide/cellulose nanofiber composite membranes. Green Chemical Engineering, 2021, 2(1): 122−131

[114] Joshi R K, Carbone P, Wang F C, et al. Precise and ultrafast molecular sieving through graphene oxide membranes. Science, 2014, 343(6172): 752−754

[115] Borges A M C, Koga G Y, Rigoli I C, et al. Electrodeposited Zn–Ni–sisal nanocrystals composite coatings — morphology, structure and corrosion resistance. Materials Research-IBERO-American Journal of Materials, 2023, 26: e20230164

[116] Lopes C D, Rigoli I C, Rovere C A D, et al. Electrodeposition and the properties of a Zn–cotton nanocrystal composite coating. Journal of Materials Research and Technology, 2022, 17: 852−864

[117] Lopes C D, Rovere C A D, Rigoli I C, et al. Electrodeposited Zn–soybean nanocrystal composite coatings: an effective strategy to produce cheaper and corrosion resistant Zn composite coatings. Journal of Materials Research and Technology, 2022, 20: 1378−1390